Experimental study of the thermal separation in a vortex tube

Yunpeng Xue, Maziar Arjomandi and Richard Kelso

Department of Mechanical Engineering
University of Adelaide, Adelaide, South Australia 5005, Australia

Abstract

The phenomenon of the temperature separation in a vortex tube has been investigated aiming to locate the real reason since its discovery. Several explanations for the separation have been proposed, however there is no well accepted explanation so far.

Understanding of the flow behaviour inside a vortex tube is an essential requirement in exploring the thermal separation. This paper reports on an experimental study in progress exploring the thermal separation in a vortex tube. Flow properties in a vortex tube are measured and used to clarify the flow structure inside the tube. The velocity distributions along the tube are presented, which are different from previous studies. Energy analysis was conducted to identify the main reason of the thermal separation in a vortex tube.

Introduction

From a single injection of compressed air, a Ranque-Hilsch vortex tube generates instant cold and hot streams at the opposite ends of the tube. Figure 1 shows the structure of a counter-flow vortex tube, which consists of a straight tube with a port for tangential injection and exits at each end. With the tangential injection of compressed gas, the cold stream is exhausted from the central exit near the inlet, and the hot stream is exhausted from the peripheral exit at the other end of the tube. Xue *et al*. [1] summarised different explanations for the thermal separation in a vortex tube. The critical analysis of these explanations reveals that there hasn't been a well-accepted explanation for the temperature separation in a vortex tube so far.
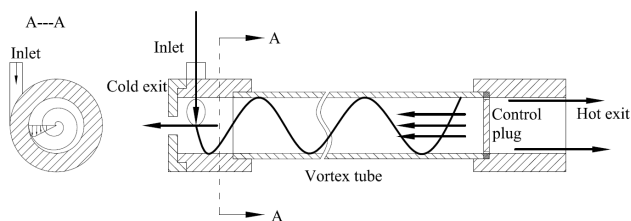

Figure 1. Working principle of a vortex tube

To identify the mechanism of thermal separation in a vortex tube, understanding of the physical process inside the tube is essential. Xue *et al.* [2] conducted a qualitative analysis of the flow behaviour in a vortex tube using flow visualization techniques, in which a flow recirculation, named the multi-circulation, was identifies, whereby part of the central flow moved outwards and returned to the hot end. Hence, they suggested that flow streams separate with different temperatures because of the sudden expansion near the inlet to generate the cold flow, and stagnation of the multi-circulation near the opposite end to generate the hot flow.

The flow properties inside the vortex tube have been studied by many researchers, in order to validate the internal flow behaviour. It was reported by Takahama [3] that the flow inside a vortex tube behaves as a forced vortex based on measurements of

the swirl velocity. To explain the existence of the secondary flow in a vortex tube, Ahlborn and Groves [4] measured both azimuthal velocity and axial velocity. Their results suggested that the flow consisted of a Rankine vortex, with a forced vortex in the centre and free vortex in the periphery. Detailed measurements of the flow in a counter-flow vortex tube, including the 3-D velocity distribution, temperature and pressure gradients, were conducted by Gao [5]. However, due to difficulties in obtaining experimental measurements inside the vortex tube, there has not been a consistent understanding of the flow behaviour, so further clarification of the flow properties is required.

In order to identify the dominant factors in the generation of separate cold and hot streams in a vortex tube, this paper presents an energy analysis of the internal flow based on the measurements of the flow properties and velocity distributions. In a specially designed large-scale vortex tube, three-dimensional velocity distributions, static temperature and static pressure inside the tube were measured and used to perform the energy analysis. It is found that the kinetic energy transferred from the central stream to the peripheral stream is not the dominant reason for the temperature drop in the vortex tube but contributes to the temperature rise near the hot end. Instead, the sudden expansion near the inlet and stagnation of the multi-circulation in the rear part of the vortex tube are the main factors in generating cold and hot streams respectively.

Experimental apparatus

Due to the strong swirling motion of the flow, the high turbulence intensity inside the vortex tube and the small dimensions of the tube, it is difficult to conduct high fidelity experimental investigations. The experimental study becomes more complicated when the measurements are taken by intrusive probes causing vortex shedding and stronger turbulence.
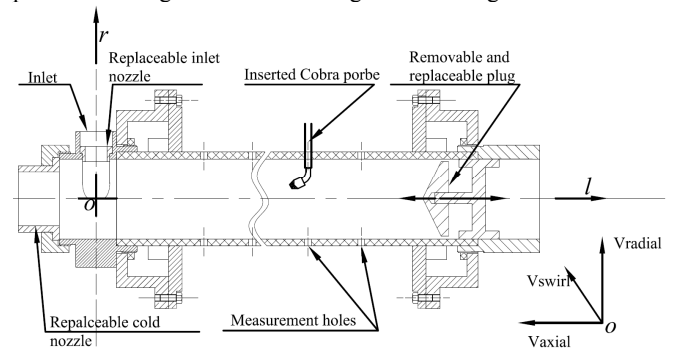

Figure 2. Structure of a counter-flow vortex tube

In order to obtain accurate quantitative observations of the flow in a vortex tube, a large-scale tube with a length of 2000mm and diameter of 60mm was employed in this work as shown in Figure 2. To allow the measurements of flow properties at different locations of the tube, 35 inline holes were drilled along the acrylic tube with a distance of 50 mm from each other. The tube

length in this experiment was fixed at 21 times of the tube diameter, i.e. L/D=21 from the inlet. A round inlet nozzle with a diameter of 6mm, a cold exit with a diameter of 14mm and a hot exit of 1 mm gap, formed by inserting a 58mm plug into the 60mm tube, were chosen based on an optimization of the temperature difference.

A Turbulent Flow Instrumentation brand Cobra probe was used to obtain 3-D velocity, static pressure and turbulence intensity profiles at different locations along the tube. The small dimension of the probe head ensured a minimum disturbance introduced to the internal flow. The probe was mounted on a manual traverse vertically with a positioning accuracy of 0.01 mm in the radial direction. By adjusting the angular position of the tube, the cobra probe was inserted through the centre of the tube, so the flow profiles were measured in the radial direction of the tube. Due to limitations in its measurement range, the cobra probe can provide accurate measurements of 3-D velocity when the flow velocity is between 2 m/s and 50 m/s. For the velocity higher than 50 m/s, the acceptable data collection by the cobra probe was less than 80%. Therefore, a Rotatable Pitot Tube (RPT) was employed to measure the pressure and velocity beyond this range. Figure 2 presents the working principle and structure of the rotatable Pitot tube, which consists of a 1mm tube sealed at one end, with a 0.2 mm measurement hole in its side and a pressure sensor connected at the other end. Thus when the tube is rotating at a constant angular velocity, the surface pressure of the tube at variable angles is collected, from which pressure and velocity profiles can be found.
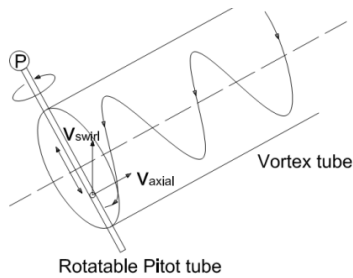

Figure 2.Principle and structure of the rotatable Pitot tube

Figure 3 shows measurements obtained by a rotatable Pitot tube positioned in a uniform flow and in a vortex tube separately. In each case, the peak pressures were obtained when the measurement hole was aligned with the oncoming flow, indicating the total pressure. From the pressure distribution in a uniform flow and knowing the static pressure, the angular phase where the surface pressure equals the static pressure was found. Hence, the flow direction and total velocity can be calculated based on these measured pressures. Therefore, using the rotatable probe, the flow angle, total and static pressure within the vortex tube could be found. Comparisons with the cobra probe showed excellent agreement.
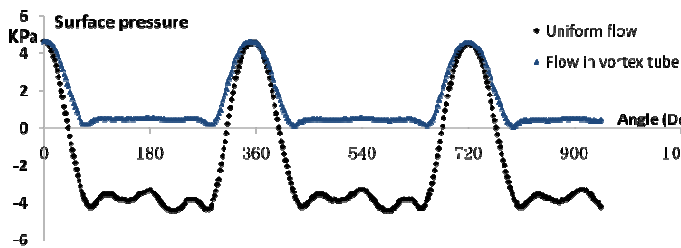

Figure 3. Pressure distributions measured by the rotatable Pitot tube in a uniform flow and flow inside the vortex tube respectively

The total temperature distribution along the vortex tube was measured using a T-type thermocouple inserted into the tube through the holes. Due to the tube dimensions and construction of the vortex tube, the temperature difference in this experiment was not as significant as it is in a commercial vortex tube. Due to the low Mach number of the flow and the relatively small temperature change in the tube, a recovery factor of 1 was assumed, based on which the static temperature was calculate.

For an experimental result, the uncertainty of a measurement can be expressed as:

$$u_{F_i} = \frac{x_i}{F} \frac{\partial F}{\partial x_i} u_{x_i} \qquad (1)$$

Where u_{F_i} is the experimental uncertainty induced by factor i, x_i is the expression of i factor, F is the mathematical expression of the experimental result, and u_{x_i} is the uncertainty of factor i. And the total experimental uncertainties can be calculated as $R_F = \pm\sqrt{\sum\left(u_{F_i}^2\right)}$. The uncertainties of the experimental results in this work are summarized below in Table 1.

Measurement result	Experimental uncertainty
Velocity from Cobra probe	0.5%
Pressure from Cobra probe	0.3%
Pressure from RPT	0.3%
Temperature	1%
Local density	1.05%
Kinetic energy density	1.3%
Exergy density	2%

Table 1. Summarized uncertainties of the experimental results

Flow properties and energy analysis

To understand the flow behaviour inside the vortex tube, the 3-D velocity distributions along the tube were measured. Figure 4 shows a typical measurement of the swirl velocity at L/D=20, in which the turbulence intensity and percentage of acceptable data are presented. The data show the existence of a high degree of swirl in the centre of the vortex tube, accompanied by high turbulence intensity. Thus, due to the high turbulence intensity, it is very difficult to measure the actual velocity components and receive acceptable data in the central part. The data also show the presence of a boundary layer at the wall of the vortex tube and this, too, is accompanied by an increase in the turbulence intensity and a lower percentage of acceptable data. The swirl velocity profile at L/D=20 is consistent with the formation of an irrotational vortex in this region. This type of motion near the hot end presents a different description of the flow structure in a vortex tube as presented in [6-8]. In the following section, the measured data of 3-D velocity distributions at several positions will be analysed, which represent a typical configuration of the flow behaviour inside the tube.
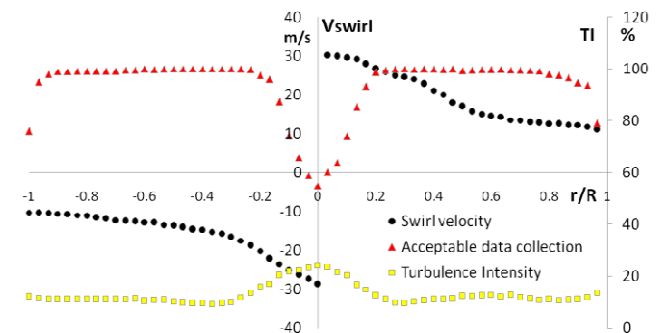

Figure 4. Swirl velocity and turbulence intensity at L/D=20

Figure 5 shows the swirl velocity distributions along the vortex tube at L/D=1, 5, 10, 15 and 20. It can be seen from the figure

that the swirling flow indicates the presence of a forced vortex near the cold exit, i.e. L/D=1, with a maximum velocity of 54.1 m/s at 3 mm from the wall and a minimum velocity close to 0 at the centre of the tube. As the flow moves to the hot end, the peripheral swirl velocity decreases and the location of the maximum velocity gradually moves to the centreline of the tube. Similarly, the swirl velocity of the central flow decreases gradually as well when it moves to the cold end. Hence, it can be summarised that the swirl flow inside the vortex tube changes from a forced vortex to an irrotational vortex model. This is contrary to the most research work in this area, in which the swirl velocity distribution along a vortex tube has been described as a forced vortex throughout the whole tube [1]. To the best of authors' knowledge the gradual transformation of the forced vortex structure to a free vortex formation along the tube has not been reported previously and is reported in this work for the first time [3-6, 9-11]. Similar observation of the velocity distribution inside the vortex tube is showed in a numerical study [12], but no comments on the transformation was reported.

It can be understood that the forced vortex formation near the cold end is the result of tangential injection of the air. When the flow moves to the hot end, due to friction near the wall of the tube, the swirl velocity component at the periphery decreases. When the flow reaches the hot end, the swirl velocity in the centre increases and forces the flow to form a free vortex. As the central flow moves to the cold end, the swirl velocity in the central region is decelerated due to the lower velocity in the peripheral layer. Part of the kinetic energy is transferred outwards by the friction between the free vortex in the centre and the peripheral flow, which improves the performance of the tube.
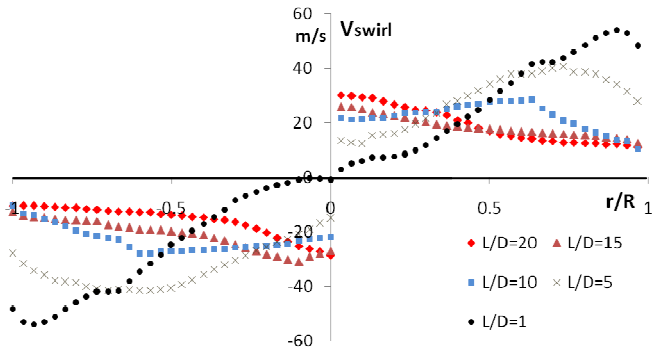

Figure 5. Swirl velocity profiles along the vortex tube

Figure 6 reports the axial velocity distributions in the vortex tube. The positive velocity in the central region indicates the flow moves to the cold nozzle and the negative velocity means the fluid flows to the hot end. The maximum axial velocity at L/D=20 appears in the centre of the tube, which shows the flow turned back along the centre by the plug. As the central flow moves to the cold end, the outwards radial flow induced by the increasing centrifugal acceleration, causes the excursion of maximum axial velocity from the centre as shown by the asymmetric profiles in the figure (L/D=15). This also indicates the formation of the above-mentioned multi-circulations near the hot end. The maximum axial velocity at L/D=5 is also located away from the centre, which can be explained by the turn back of the flow in the front part of the tube as described in [1, 2]. It can be concluded from the figure that the cold stream exhausted from the cold nozzle is more than the flow moving towards the cold end near the hot end. This supports the statement that the cold stream mainly comes from the turn-back flow near the injection [2]. It should be noted that the quality of the data collection near the inlet is relative poor due to the high injection velocity and sudden expansion near the inlet, so a more accurate measurement of the velocity near the inlet is recommended.
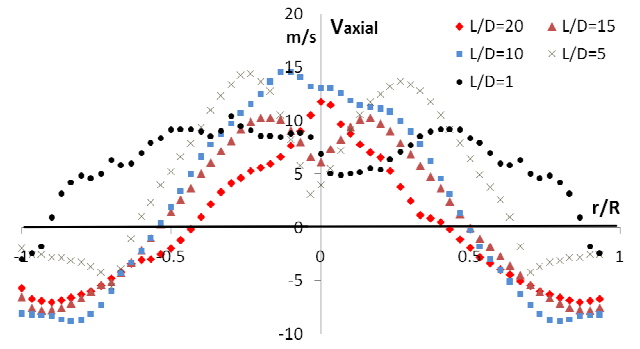

Figure 6. Axial velocity profiles along the vortex tube

Figure 7 shows the radial velocity distribution along the tube, which has not been investigated in previous studies due to its small magnitude. Positive velocity in the figure indicates that the flow is moving outwards. Hence, the radial velocity at L/D=1 shows that flow is moving to the centre and indicates the existence of the turn-back flow in front part of the tube. At L/D=5, 10 and 20, the swirling flow departs from the centre and moves upwards, which is indicated by the positive velocity in the central region of the tube. These offsets of the radial velocity at L/D=10, 15 and 20, can be explained by the asymmetry of the flow in the vortex tube with single injection as stated in [2]. At L=15D, corresponding to the position of the multi-circulation, the outwards flow from the centre indicates the formation of the multi-circulation. However, due to the unsymmetrical flow generated by a single injection and small magnitude of the radial velocity, accurate measurements of the radial velocity in a vortex tube with symmetrical injections is recommended, since this will provide a more reliable description of the internal flow structure without the complicating influence of asymmetry.
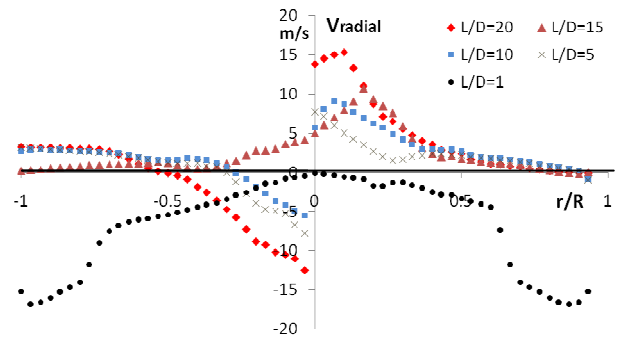

Figure 7. Radial velocity profiles along the vortex tube

For a compressible flow, exergy is always used instead of energy, which contains the component of entropy change. In order to perform a detailed analysis of the exergy distribution inside the vortex tube, the density of the local fluid was used instead of the control volume, which indicates the exergy density inside the tube. Therefore, the equation is written in the following form:

$$ex_i = \rho_i C_p (T_i - T_o) + \rho_i \left(\frac{1}{2} \bar{v}_i^2 + \frac{3}{2} (v' I_{uvw})_i^2 \right)$$
$$- \rho_i T_o \left(\frac{C_p \ln T_i}{T_o} - R \ln \frac{P_i}{P_o} \right) \tag{2}$$

Here, ρ_i is the local density and calculated using the state equation, C_p is the specific heat at constant pressure, T and P represent the static temperature and static pressure, the subscripts "i" and "o" represent the instant and reference conditions of a process separately, $\bar{v}$ is the time-averaged total velocity, v' is time-varying velocity fluctuating component, I_{uvw} is the overall turbulence intensity, and R is the universal gas constant.

Figure 8 presents the calculated exergy density inside the vortex tube at different locations. It is shown that the exergy density in

the peripheral region decreases dramatically from the inlet, which is caused by the filling of the central part of the vortex tube by the peripheral flow. At $l/D=1$, the decrease of the exergy density in the radial direction also indicates the formation of the cold core. Towards the hot end, the radial gradient of exergy density becomes constant. Heat transfer from the wall of the tube to the ambient air causes a gradual decrease in exergy density from approximately $l/D=10$ to the hot end. The outer layer of the peripheral flow at the hot end is exhausted from the hot exit and the inner part of the peripheral flow is forced back by the plug towards the cold end through the central region of the tube. Therefore, the lower exergy density of the central flow at the hot end ($l/D=20$) is caused by the forced-back central flow from the peripheral part. As the central flow moves to the cold end, the exergy density decreases and reaches the minimum value at the cold end. At the peripheral region of the flow, the slightly reduced exergy density near the hot end indicates that there is no energy transferred outwards and that the temperature rise near the hot end is mainly caused by the mixture and partial stagnation of the axial flow via the structure of multi-circulation.

Overall, in the central region, none of the energy transferred outwards near the cold end indicates the governing factor for temperature drop in a vortex tube is the effect of sudden expansion. Heat transferred from the tube to ambient air causes the reduction of exergy density in the peripheral part of the flow from the cold end to the hot end. Energy transferred from the central free vortex flow outwards to the periphery has a positive influence on the temperature rise at the hot end. The slightly decreased exergy density of the peripheral flow near the hot end indicates that the stagnation and mixture of the multi-circulation are the dominant factors in the temperature rise. However, due to the limited temperature difference in this experiment, it is not available to have an accurate calculation of the temperature rise because of the energy transferred outwards.
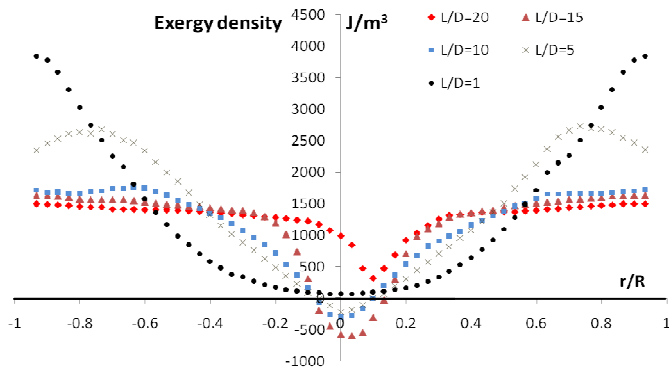

Figure 8. Exergy density profiles within the vortex tube

Conclusion

Although several explanations for the temperature separation in a vortex tube have been proposed, due to the complexity of the internal flow, there has not been a well accepted explanation and the physical process inside the vortex tube remains unclear. This ongoing research focuses on the flow properties inside a counter-flow vortex tube aiming to locate the dominant reason for the temperature separation in a vortex tube.

This experimental study presents detailed measurements of the flow properties inside a counter-flow vortex tube. The three-dimensional velocity distributions inside the vortex tube lead to a

new understanding of the flow behaviour in the vortex tube. It is noted that in the central region of the tube, the irrotational vortex at the hot end was transformed to a forced vortex near the injection and kinetic energy is only transferred outwards from the hot end to the cold end. The locations of the maximum axial velocity indicate the change of the flow structure and support the hypothesis of a multi-circulation as stated in [1, 2].

Using the detailed flow properties, the exergy density inside the vortex tube is calculated and provides positive support for the proposed hypothesis in [1]. Sudden expansion near the cold end is considered as the main reason for the temperature drop, since there is no energy transferred outwards from the central region. The slightly changed exergy density near the hot end indicates that the temperature rise is mainly due to the stagnation of the structure of multi-circulation. Kinetic energy is transferred outwards from the irrotational vortex in the central region and contributes to the temperature rise in the periphery near the hot end.

Reference

[1] Y. Xue, M. Arjomandi, R. Kelso, A critical review of temperature separation in a vortex tube, Experimental Thermal and Fluid Science, 34 (2010) 1367-1374.
[2] Y. Xue, M. Arjomandi, R. Kelso, Visualization of the flow structure in a vortex tube, Experimental Thermal and Fluid Science, 35 (2011) 1514-1521.
[3] H. Takahama, Studies on vortex tubes, Bull. JSME, 8 (1965) 433-440.
[4] B. Ahlborn, S. Groves, Secondary flow in a vortex tube, Fluid Dynamics Research, 21 (1997) 73-86.
[5] C.M. Gao, K.J. Bosschaart, J.C.H. Zeegers, A.T.A.M. De Waele, Experimental study on a simple Ranque-Hilsch vortex tube, Cryogenics, 45 (2005) 173-183.
[6] U. Behera, P.J. Paul, K. Dinesh, S. Jacob, Numerical investigations on flow behaviour and energy separation in Ranque-Hilsch vortex tube, International Journal of Heat and Mass Transfer, 51 (2008) 6077-6089.
[7] S. Eiamsa-ard, P. Promvonge, Numerical investigation of the thermal separation in a Ranque-Hilsch vortex tube, International Journal of Heat and Mass Transfer, 50 (2007) 821-832.
[8] W. Fröhlingsdorf, H. Unger, Numerical investigations of the compressible flow and the energy separation in the Ranque-Hilsch vortex tube, International Journal of Heat and Mass Transfer, 42 (1999) 415-422.
[9] T. Dutta, K.P. Sinhamahapatra, S.S. Bandyopdhyay, Comparison of different turbulence models in predicting the temperature separation in a Ranque-Hilsch vortex tube, International Journal of Refrigeration, 33 (2010) 783-792.
[10] O.V. Kazantseva, S.A. Piralishvili, A.A. Fuzeeva, Numerical simulation of swirling flows in vortex tubes, High Temperature, 43 (2005) 608-613.
[11] T. Farouk, B. Farouk, Large eddy simulations of the flow field and temperature separation in the Ranque-Hilsch vortex tube, International Journal of Heat and Mass Transfer, 50 (2007) 4724-4735.
[12] A. Secchiaroli, R. Ricci, S. Montelpare, V. D'Alessandro, Numerical simulation of turbulent flow in a Ranque-Hilsch vortex tube, International Journal of Heat and Mass Transfer, 52 (2009) 5496-5511.